Controlled Reduction of the Acid Site Density of SAPO-34 Molecular Sieve by Means of Silanation and Disilanation

Filip D. P. Mees,*,† Pascal Van Der Voort,† Pegie Cool,† Luc R. M. Martens,‡ Marcel J. G. Janssen,‡ An A. Verberckmoes,‡ Gordon J. Kennedy,§ Richard B. Hall,§ Kun Wang,§ and Etienne F. Vansant†

University of Antwerpen, Universiteitsplein 1, 2610 Wilrijk, Belgium, ExxonMobil Chemical Europe, Hermeslaan 2, B-1831 Machelen, Belgium, and ExxonMobil Research and Engineering Company, Annandale, New Jersey 08801

Received: December 3, 2002; In Final Form: February 3, 2003

SAPO-34 has been modified by silanation and disilanation reactions. The acidic properties of these modified SAPOs have been characterized by IR measurements. The bands of the bridging hydroxyls at 3600 and 3625 cm^{-1} show a gradual decrease in intensity with increasing silane or disilane loading. The band intensity of the P−OH group at 3675 cm^{-1} remains unaffected. The silanation process can be monitored (i) spectroscopically through the characteristic IR band of Si−H at 2250 cm^{-1} and (ii) analytically by the changes in the H_2/SiH_4 ratio during the modification. CD_3CN has been used as an IR spectroscopic probe to elucidate the changes in Brønsted and Lewis acidity of the modified SAPO-34. The intensity of the C≡N absorption band at 2320 cm^{-1}, which is attributed to CD_3CN adsorbed on Lewis acid sites, increases relative to the band at 2290 cm^{-1} (Brønsted acidity). This indicates that Brønsted acid sites are irreversibly transformed into Lewis acid sites after silanation reactions on the SAPO-34. ^1H and ^{29}Si MAS NMR confirm that the silanes react with the Brønsted acid sites resulting in silicon incorporation and silanol formation. Methanol adsorption capacity measurements indicate that silanation and disilanation reactions cause a significant reduction of the void volume of the SAPO-34 cages without creating diffusion limitations. The ethylene/ethane and propylene/propane selectivity ratios in the MTO reaction (methanol-to-olefins) increase as a function of the (di)silane loading, while the amount of coke on the SAPO-34 decreases linearly with increasing (di)silane loading.

Introduction

In 1982 the family of aluminosilicate zeolites was extended by the discovery of the aluminophosphate molecular sieves.[1,2] In these crystalline microporous aluminophosphates ($AlPO_4$'s), the tetrahedral (T) sites are occupied alternately by Al^{3+} and P^{5+} ions. By substituting a Si for a P, a negative charged framework is obtained so that Brønsted acidity can be introduced. Silicon-substituted $AlPO_4$'s are designated SAPO-n where n represents a structure type.[3] SAPO-34, which is structurally analogous to the zeolitic mineral chabazite,[4] is acknowledged to be a powerful catalyst for the MTO-process, exhibiting high light olefin selectivities. The catalytic performance of these SAPO molecular sieves is believed to be not only governed by the precise framework structure but also by the acid site strength (distribution) and the acid site density.[5] A way of altering the acidic properties of AlPO and SAPO molecular sieves consists of introducing bivalent cations (such as Co^{2+}) on framework positions replacing Al^{3+}. These modifications result in MeAPO's and MeAPSO's. Several authors have studied the acidic[6,7] and catalytic[8] properties of these materials.

This contribution assesses the modification of the SAPO-34 acidic sites by postsynthesis modification techniques using SiH_4 and Si_2H_6. In this way, the chemical composition and/or structural characteristics of the substrate can be altered over a wide range and in a continuous manner without affecting the original zeolite type. The aim is to study the influence of the acid site strength and the acid site density of the SAPO-34 on the MTO performance, without changing the SAPO's framework. The silanation and disilanation of zeolites was developed by Vansant et al.[9−13] and can be seen as a three-step process.

1. Primary reaction: chemisorption of SiH_4. The silane molecules react with acidic −OH groups. One H_2 molecule is liberated.

$$\equiv Si-OH + SiH_4 \rightarrow \equiv Si-O-SiH_3 + H_2$$

2. Secondary reactions: The chemisorbed hydride compound reacts further with other acidic −OH groups. Another H_2 molecule is liberated.

$$\equiv Si-O-SiH_3 + HO-Si\equiv \rightarrow \equiv Si-O-SiH_2-O-Si\equiv + H_2$$

3. Hydrolysis reactions: The remaining hydride bonds are hydrolyzed with water to form Si−OH groups, again releasing H_2.

$$\equiv Si-O-SiH_3 + 3H_2O \rightarrow \equiv Si-O-Si(OH)_3 + 3H_2$$

$$\equiv Si-O-SiH_2-O-Si\equiv + 2H_2O \rightarrow \equiv Si-O-Si(OH)_2-O-Si\equiv + 2H_2$$

* Corresponding author. E-mail: filip.mees@ua.ac.be.
† University of Antwerpen.
‡ ExxonMobil Chemical Europe.
§ ExxonMobil Research and Engineering Company.

10.1021/jp0276045 CCC: $25.00
Published on Web 03/18/2003

The ratio R of H_2 liberated over SiH_4 or Si_2H_6 chemisorbed is a measure for the extent of the reaction. Per SiH_4 molecule a maximum of four H_2 molecules can be liberated. The disilanation of zeolites follows a similar reaction pathway, although more side reactions have to be considered.

1. Chemisorption of Si_2H_6

$$Si_2H_6 + HO-Si\equiv \rightarrow H_5Si_2-O-Si\equiv + H_2 \qquad R = 1 \quad \text{(P1)}$$

$$Si_2H_6 + 2HO-Si\equiv \rightarrow 2\,H_3Si-O-Si\equiv + H_2 \qquad R = 1 \quad \text{(P2)}$$

2. Secondary reactions

$$\equiv Si-O-Si_2H_5 + xHO-Si\equiv \rightarrow (\equiv Si-O-)_{(1+x)}Si_2H_{(5-x)} + xH_2 \qquad R = 1 + x \quad \text{(S1)}$$

$$\equiv Si-O-SiH_3 + xHO-Si\equiv \rightarrow (\equiv Si-O-)_{(1+x)}SiH_{(3-x)} + xH_2 \qquad R = 1 + x \quad \text{(S2)}$$

$$\equiv Si-O-Si_2H_{(m+n)} + (x+y+2)HO-Si\equiv \rightarrow (\equiv Si-O\text{-})_{(2+x)}SiH_{(m-x)} + (\equiv Si-O-)_{(1+y)}SiH_{(n-y)} + (x+y+1)H_2 \qquad R = 2 + x + y \quad \text{(S3)}$$

3. Hydrolysis reactions

$$\equiv Si-H + H_2O \rightarrow \equiv Si-OH + H_2 \qquad R \leq 7 \quad \text{(H1)}$$

$$\equiv Si-Si\equiv + 2H_2O \rightarrow 2\,\equiv Si-OH + H_2 \qquad R \leq 7 \quad \text{(H2)}$$

Theoretically, seven H_2 molecules can be liberated per Si_2H_6 molecule.

The changes in acidity introduced by (di)silanation are investigated with IR spectroscopy. Deuterated acetonitrile has been used as a probe molecule for these experiments since the ν(C≡N) stretching IR absorption band is very sensitive to the interaction between the molecule and the acid sites of the zeolite.[14] The characteristic shifts of the ν(C≡N) modes allow discrimination between Brønsted and Lewis acidity. The silanated and disilanated SAPO-34's were further studied by ^{1}H and ^{29}Si MAS NMR and tested on their catalytic performance in the MTO reaction.

Experimental Section

SAPO-34, synthesized with TEAOH as a templating agent, was kindly provided by ExxonMobil. The samples were calcined at 625 °C for 4 h under ambient air in order to remove the template. Modification of the calcined samples was performed in a dynamic gas-volumetric adsorption apparatus, as described previously.[15] After the samples were outgassed at 300 °C overnight, SiH_4 or Si_2H_6 were contacted with the SAPO-34 at 150 °C in the evacuated system. The reaction was monitored by measuring the ratio of H_2 evolved over the amount of SiH_4 or Si_2H_6 chemisorbed. After the unreacted SiH_4 was evacuated, the hydride bonds were hydrolyzed by contacting the silanated sample with H_2O at 150 °C. The hydrolysis reaction was monitored by measuring the amount of H_2 evolved. The modified sample was subjected to a dehydration treatment at 625 °C to remove residual water.

DRIFT spectra were recorded on a Nicolet Nexus FTIR spectrometer equipped with an in situ DRIFTS cell (SpectraTech) and an MCT detector. The samples were mixed with KBr (95% KBr; 5% SAPO). The measurements were performed in a vacuum at 200 °C after degassing the SAPO-34 in situ for 15 min. The spectral resolution was 4 cm^{-1}.

Transmission spectra were measured on a Nicolet 20SX spectrometer equipped with a vacuum cell and a DTGS detector. Self-supporting disks, each with a thickness of 20 mg/cm^2, were used. After they were outgassed in a vacuum at 300 °C overnight, the samples were contacted with deuterated acetonitrile in a vacuum at room temperature (15 min). The spectra were recorded after evacuation for 15 min at room temperature ($P = 10^{-3}$ mbar). Five hundred scans were coadded with a spectral resolution of 4 cm^{-1}. Desorption of CD_3CN was carried out at 25, 50, 75, 100, 150, and 200 °C for 15 min.

The ^{1}H and ^{29}Si MAS NMR measurements were carried out at room temperature on a Bruker AMX360 wide bore spectrometer equipped with a solids accessory operating at a static magnetic field of 8.4 T, corresponding to Larmor frequencies of 360.1 and 71.6 MHz, respectively. The ^{29}Si spectra were recorded using single pulse Bloch decay and cross polarization techniques on samples loaded in 7.5-mm (o.d.) MAS PENCIL rotors and spinning at the magic angle at rates of about 5 kHz. The single-pulse experiments were conducted with high power ^{1}H decoupling during data acquisition using 5-μs $\pi/2$ pulses and a 15-s pulse delay, and 6000−8000 scans were collected. The cross-polarization experiments were conducted with a 4-μs $\pi/2$ ^{1}H pulse, 3.5-ms contact time, and a 2-s recycle delay, while 30 000−40 000 transients were collected. The ^{1}H MAS NMR spectra were recorded with a Bruker 4-mm (o.d.) MAS probe using 10-kHz spinning, 3.0-μs $\pi/2$ pulses, and a 30-s pulse delay, and 32 scans were collected. To avoid moisture, which seriously affects the quality of the ^{1}H NMR spectra and could overwhelm the ^{1}H NMR signal, the samples were evacuated at 400 °C/10 h, then capped under N_2 prior to the ^{1}H NMR measurements. The capped rotors were kept in a drybox until the ^{1}H NMR data collection commenced. Chemical shifts for ^{1}H and ^{29}Si were calibrated using TMS ($\delta_H = 0$ ppm; $\delta_{Si} = 0$ ppm).

Methanol adsorption measurements were performed on a gravimetric adsorption apparatus. The samples were degassed in a dynamic vacuum for 30 min and exposed to methanol vapor at room temperature. The variation in weight is a measure for the amount of methanol adsorbed.

The MTO reaction was performed in a stainless steel, fixed-bed continuous reactor. Pure methanol was used as feed. Prior to testing, the SAPO-34 was activated in a muffle furnace at 625 °C (5 °C/min; 4 h). A 40−60 Mesh sieve fraction was diluted with SiC. The reaction is carried out at 450 °C, a reactor pressure of 103 kPa and a WHSV (weight hourly space velocity) of 26 g/g hr. Reaction products were analyzed with an on-line GC. Methanol conversion is calculated as 100 − (wt % methanol + wt % dimethyl ether) left in the product.

Results and Discussion

Silanation and Disilanation of SAPO-34. The kinetics of the silanation and that of H_2 evolution from the SAPO-34, degassed at 300 °C overnight, are shown in Figure 1. A dose of 0.55 mmol/g of SiH_4 was reacted at 150 °C with the calcined SAPO-34, resulting in complete chemisorption after approximately 1000 min. The corresponding evolution of H_2 (0.546 mmol/g) was the same as the amount of silane chemisorbed indicating that no significant secondary reactions took place. At this stage a dose of water was introduced, still at 150 °C, and the amount of H_2 evolved slowly rose to 1.82 mmol/g after 2600 min, resulting in a ratio of H_2/SiH_4 of 3.3. After the hydrolysis reactions, the modified SAPOs were outgassed at 625 °C and used for the IR measurements.

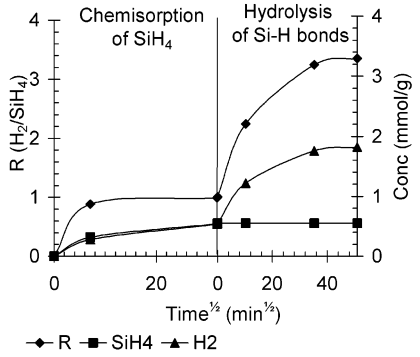

Figure 1. Variation of chemisorbed SiH_4, liberated H_2 and *R*-value during the silanation of SAPO-34.

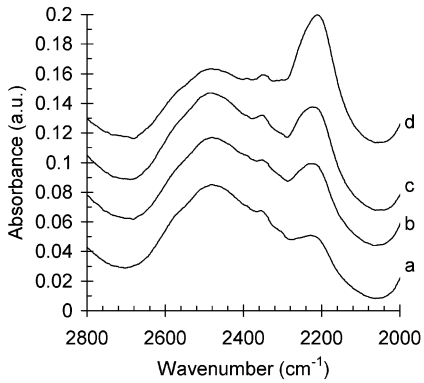

Figure 2. DRIFT spectra of silanated SAPO-34 after primary chemisorption: (a) 0, (b) 0.21, (c) 0.55, and (d) 0.78 mmol SiH_4/g SAPO-34.

Other samples were prepared in the same way, resulting in modification degrees ranging from 0.2 to 0.8 mmol/g. After the primary chemisorption reaction, the *R*-value was always close to unity for the silanation reactions. This indicates that for the silanation of SAPO-34, secondary reactions do not occur at temperatures below 150 °C. The final *R*-value (defined as the amount H_2 released over the amount SiH_4 chemisorbed) was always between 3 and 3.5 for the silanated SAPO-34. Theoretically, four bonds can be oxidized in a SiH_4 molecule, resulting in a *R*-value of 4. IR data indicated that after the hydrolysis reactions at 150 °C, there remained some Si−H bonds that did not react. These remaining Si−H bonds were therefore oxidized in a final calcination step. For the disilanation of the SAPO-34, higher *R*-values were observed because more bonds per molecule can be oxidized. The final *R*-value was approximately 6, for disilanation degrees ranging from 0.2 to 0.6 mmol/g. Theoretically, seven bonds can be oxidized.

Infrared Measurements. Figures 2 and 3 show the DRIFT spectra of the silanated SAPO-34 after chemisorption of SiH_4 and after the hydrolysis reactions.

After silane chemisorption (Figure 2), the appearance of an absorption band at around 2250 cm^{-1} is observed, whose intensity increases with the SiH_4 loading. This peak is attributed to the Si−H stretching vibration and disappears after the hydrolysis reactions followed by a thermal treatment.

Figure 3 depicts the spectra of the silanated SAPO-34 after oxidation of the Si−H bonds. The bands at 3600 and 3625 cm^{-1}, assigned to bridged hydroxyls,[16] gradually decrease with increasing SiH_4 content. The intensity of the peak at 3675 cm^{-1}, which is attributed to P−OH groups, remains constant after the silanation of SAPO-34. This indicates that the SiH_4 molecules primarily react with Brønsted acid sites present in the SAPO-34 cages. The P−OH groups, which are only weakly acidic,[17]

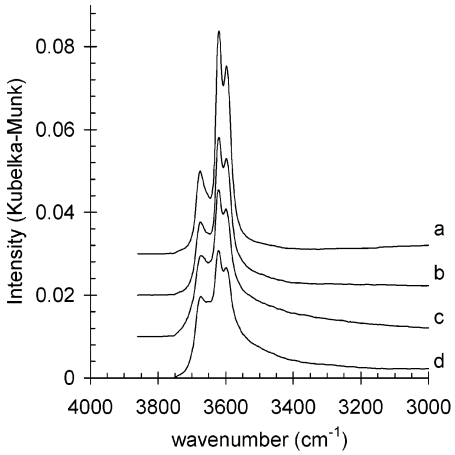

Figure 3. DRIFT spectra of silanated SAPO-34 after hydrolysis: (a) 0, (b) 0.21, (c) 0.55, and (d) 0.78 mmol SiH_4/g SAPO-34.

apparently are unreactive to SiH_4. This is due to the fact that the silanation is a nucleophilic substitution reaction in which the SiH_4 molecule is the electrophile. When the acidity of structural −OH groups is too low, the ionic character and the electron density on the oxygen atom are insufficient to substitute SiH_4 for H. The IR spectra of SAPO-34 after the chemisorption of disilane showed the Brønsted acidity to decrease with increasing disilane loading. The peak area of the Brønsted bands, however, decreased approximately twice as much compared to the same silane loading, indicating that each disilane molecule irreversibly poisons two acid sites.

The acidic sites of the SAPO-34 after (di)silanation reactions were further investigated using deuterated acetonitrile as a probe molecule. Acetonitrile is an attractive probe molecule since it allows the investigation of both Lewis and Brønsted acidity. The stretching mode of the protonic sites of the molecular sieve shifts and the C≡N stretching vibration is influenced by interaction with the acidic sites. Characteristic shifts of the ν(CN) modes can be used to discriminate between the Brønsted and Lewis sites as well as between Lewis centers of different chemical nature.[18] Figure 4A shows the spectra of a SiH_4-modified SAPO-34 (0.5 mmol/g) with adsorbed CD_3CN as a function of the desorption temperature. In the region ranging X from 4000 to 2500 cm^{-1}, the changes in the OH stretching vibrations of the SAPO due to the CD_3CN adsorption can be studied.

It is obvious that the bands at 3741, 3675, and 3625−3600 cm^{-1}, attributed to Si−OH, P−OH and bridged hydroxyls, respectively, disappear after acetonitrile adsorption. A so-called (A,B,C) trio of bands appears at around 2900, 2500, and 1600 cm^{-1}, typical for strong H complexes in vapors, liquids, and solids.[19−21] These bands can thus be attributed to Brønsted hydroxyls at which acetonitrile is adsorbed. Their intensity decreases with increasing SiH_4 content (not shown in this figure). The IR region between 2500 and 2000 cm^{-1} shows the changes observed for the acetonitrile vibrations. A band at ca. 2320 cm^{-1} is related to the C≡N interaction with the Al^{III} Lewis acid sites.[22] The band at ca. 2290 cm^{-1} is due to the C≡N stretching mode of acetonitrile sorbed on the bridging Si−OH−Al groups (Brønsted acid sites).[14] The band at 2265 cm^{-1}, which is clearly seen in the top spectrum of Figure 4A, originates from physically adsorbed acetonitrile. This band is very close to the absorption band of the free acetonitrile.[23] Furthermore, two weak bands can be observed which are associated with the CD_3 group. One weak band at 2114 cm^{-1} is due to the symmetric vibration of the CD_3,[24] the other band at 2250 cm^{-1}, which is very weak,

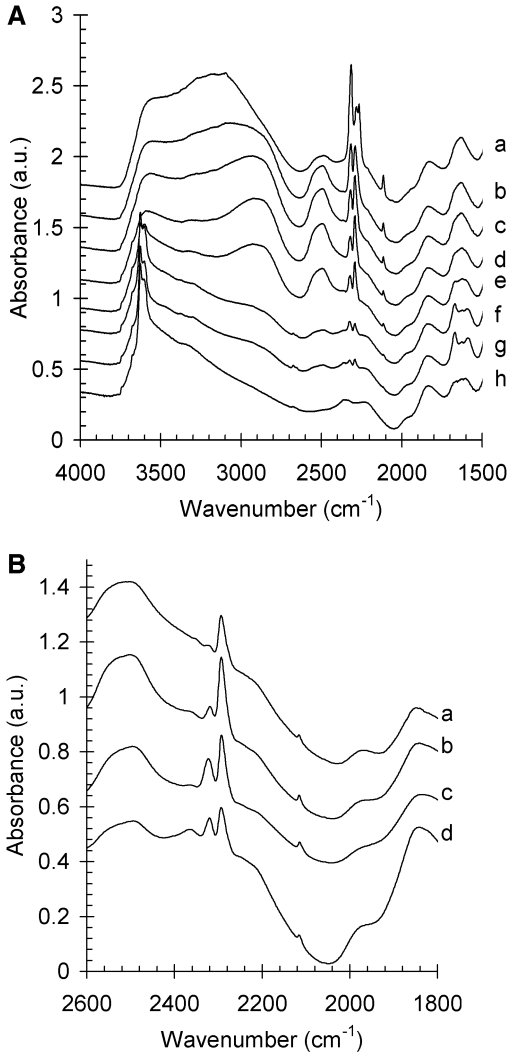

Figure 4. A: IR spectra of silanated (0.55 mmol/g) SAPO-34 with adsorbed CD_3CN: (a) after adsorption of CD_3CN; (b−g) after desorption of CD_3CN at 25, 50, 75, 100, 150, and 200 °C, respectively; (h) before adsorption of CD_3CN. B: IR spectra of SAPO-34 with adsorbed CD_3CN as a function of the silane loading: (a) 0, (b) 0.21, (c) 0.55, and (d) 0.78 mmol SiH_4/g SAPO-34 (spectra were recorded after desorption at 100 °C in a vacuum).

TABLE 1: Characteristic Frequencies of CD_3CN Adsorbed on Molecular Sieves

	wavenumber (cm^{-1})	assignment
	2114	δ_s (CD_3)
	2250	δ_{as} (CD_3)
	2265	ν (CN) condensed
CD_3CN-related	2278	ν (CN) Si−OH terminal
	2280−2284	ν (CN) P−OH
	2300	ν (CN) Brønsted
	2320−2332	ν (CN) Lewis
	2600	ν (OH) Si−OH−Al
OH-related	3100	ν (OH) P−OH
	3300	ν (OH) Si−OH

is due to the asymmetric vibration of the CD_3 of acetonitrile.[25] The characteristic frequencies of CD_3CN adsorbed on different sites are summarized in Table 1.

The interaction between the CD_3CN and the Brønsted acid sites of the SAPO-34 samples is very strong. Both on the parent and the silanated samples, acetonitrile only starts to desorb after heating at 100 °C in a vacuum. The band at 2280−2292 cm^{-1}, which is attributed to the Brønsted-bonded acetonitrile, shifts to higher frequencies during desorption of the acetronitrile. This

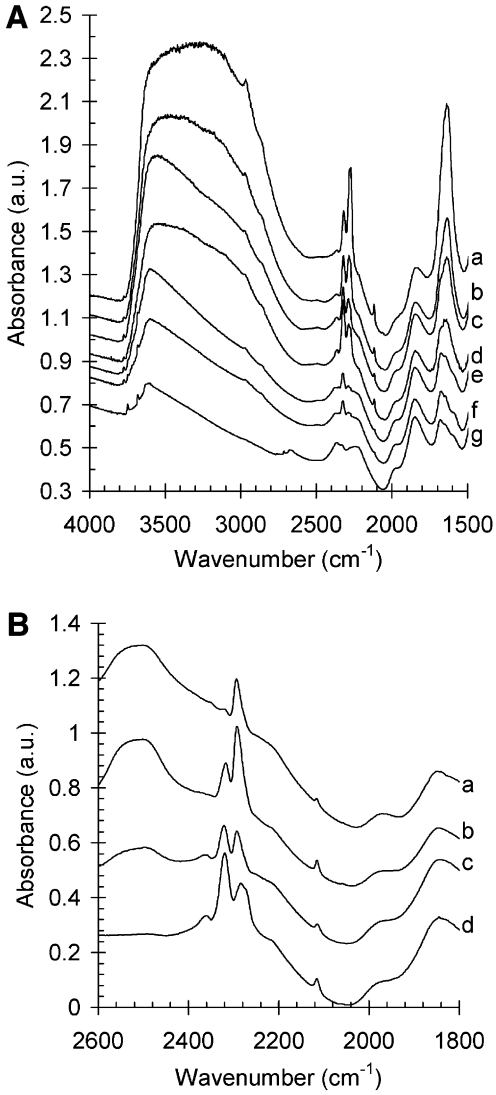

Figure 5. A: IR spectra of disilanated (0.60 mmol/g) SAPO-34 with adsorbed CD_3CN: (a−f) after desorption of CD_3CN at 25, 50, 75, 100, 150, and 200 °C, respectively; (g) before adsorption of CD_3CN. Figure 5B: IR spectra of SAPO-34 with adsorbed CD_3CN as a function of the disilane loading: (a) 0, (b) 0.2, (c) 0.4, and (d) 0.6 mmol Si_2H_6/g SAPO-34 (spectra were recorded after desorption at 100 °C in a vacuum).

shift was attributed to the contribution of acetronitrile adsorbed on P−OH groups at high loading.[6] Figure 4B depicts the spectra of the CD_3CN-loaded, modified SAPO-34's after desorption at 100 °C. The parent SAPO-34 contains almost no strong Lewis acid sites. The intensity of the band at 2320 cm^{-1} is very low compared to the Brønsted-bonded acetonitrile band at 2290 cm^{-1}. These Lewis sites are a result of nonframework Al species. The other spectra of Figure 4B show the acetronitrile bands of SAPO-34 with increasing SiH_4. It is obvious from these spectra that the relative contribution of the Lewis-bonded acetronitrile increases with increasing extra Si content. Also the strength of the interaction of CD_3CN with these newly formed Lewis sites has increased. While for the unmodified SAPO-34 all the acetonitrile adsorbed on the Lewis sites is desorbed at 100 °C, the modified SAPO's still show an important amount of Lewis-bonded CD_3CN at this temperature. This suggests that the Lewis acidity generated from silanation of the SAPO-34 is not caused by the same extraframework Al species, as in case of the unmodified SAPO-34. It is proposed that the $(AlO)_3Si$−OH−*Al* Brønsted acidic group is transformed into a $(AlO)_3Si$-

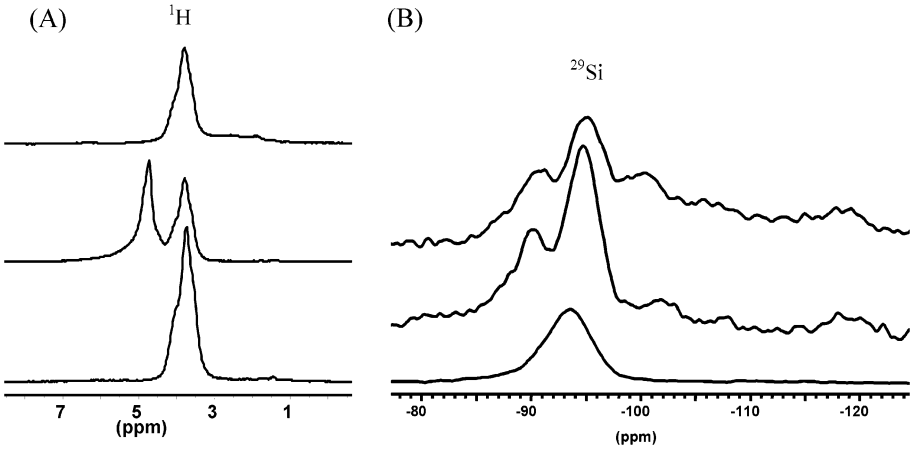

Figure 6. ^{1}H and ^{29}Si MAS NMR spectra of silanated SAPO-34: spectra of the parent (bottom) SAPO-34, the same SAPO-34 after the primary chemisorption of (middle) SiH_4, and this silanated sample after oxidation with (top) N_2O.

TABLE 2: Weighed Average Product Selectivities of SAPO-34 after Silanation and Disilanation Reactions

SiH_4/Si_2H_6	Si content mmol/g	CH_4	$C_2^=$	C_2^0	$C_3^=$	C_3^0	C_4-C_6	coke	$C_2^=/C_2^0$	$C_3^=/C_3^0$
parent	0	0.85	32.3	0.82	41.7	3.09	21.2	22.0	39.3	13.5
SiH_4	0.2	0.82	30.6	0.62	40.4	3.41	24.1	20.4	49.2	11.9
Si_2H_6	0.4	1.16	32.5	0.58	39.5	2.17	24.0	15.7	56.0	18.2
SiH_4	0.5	1.01	31.9	0.65	40.1	2.85	23.4	18.6	48.9	14.1
Si_2H_6	0.8	0.95	26.5	0.45	41.3	2.06	28.8	13.2	58.9	20.0
Si_2H_6	1.2	0.96	25.3	0.37	39.1	1.53	32.8	10.1	68.6	25.5

(OSi) group. After this reaction, the *Al* that was in coordination with the Si−OH remains as a coordinatively unsatured species and can act as a Lewis acid site. The reaction is studied in further detail by ^{29}Si MAS NMR and ^{1}H MAS NMR. Upon increasing the Si content (from SiH_4), the spectra also show that, the intensity of the band at 2500 cm^{-1}, associated with strongly complexed H^+ Brønsted sites, decreases. This further suggests that silanation of SAPO-34 selectively reduces strong Brønsted acidity.

Figure 5A shows the IR spectra of Si_2H_6-modified SAPO-34 (0.6 mmol/g) at which CD_3CN was adsorbed and desorbed at increasing temperatures.

The spectrum of the sample before CD_3CN was adsorbed, shows that the intensity of the Brønsted bands at 3600−3625 cm^{-1} is much lower after the disilanation of SAPO-34 than after the silanation (Figure 4A, bottom spectrum) for comparable amounts of modifying agent. Band integration suggested that the decrease in Brønsted acidity is approximately twice as high after disilanation than after silanation of the SAPO-34. This indicates that one disilane molecule reacts dissociatively with the acid sites, resulting in the modification of two acid sites. The same observation was made in the DRIFT spectra of these samples. The strong decrease in acidity is further confirmed by the spectra of the SAPO-34 with adsorbed CD_3CN shown in Figure 5A.

The bands at around 2900 and 2500 cm^{-1}, associated with strong H^+ complexes, are not observed after acetonitrile adsorption. The intensity of the band at 2290 cm^{-1} decreases after the modification. The relative intensity of the band at 2320 cm^{-1}, which is attributed to Lewis-bonded acetonitrile, strongly increases after modification with Si_2H_6.

Figure 5B shows the spectra of disilanated SAPO-34 with adsorbed CD_3CN after desorption at 100 °C as a function of the disilanation degree. It is obvious that the relative increase in Lewis acidity is much higher after disilanation than after silanation reactions for comparable modification degrees, i.e., comparable amounts of modifying agent. The general scheme for the chemisorption reactions of disilane was proposed by Yan et al.[12] and is summarized in the Introduction. For the disilanation of a Large Port mordenite, it was found that the primary chemisorption mainly occurs following mechanism P1, although the authors suggested that the preferential reactions are affected by the structure of the zeolite and by the reaction conditions, especially the reaction temperature. For the disilanation of a SAPO-34, the data presented in Figure 5A,B suggest that an important part of the incorporated Si−Si bonds are broken in a reaction alike mechanism P2. After the cleavage of the ≡Si−Si≡ bond and the subsequent chemisorption of two SiH_3 entities, further (hydrolysis) reactions follow the same reaction course as the silanation. In this way, equimolar amounts of Si_2H_6 and SiH_4 result in a different amount of modified Brønsted sites and of new Lewis sites in the SAPO-34. If however the amount of incorporated Si is considered, silanated and disilanated SAPO-34's show comparable IR characteristics. The similarity between silanation and disilanation is further evidenced by catalytic testing (vide infra).

NMR Characterization. Figure 6A,B show the ^{1}H and ^{29}Si MAS NMR spectra of silanated SAPO-34.

Shown in Figure 6A are the ^{1}H MAS NMR spectra of the parent SAPO-34 (bottom), the same SAPO-34 after the primary chemisorption of SiH_4 (middle), and this silanated sample after oxidation with N_2O (top). The ^{1}H MAS NMR spectrum of the parent sample shows peaks centered at 3.8 ppm (ppm from TMS) attributed to acidic protons. After the primary chemisorption of SiH_4, the intensity of this peak strongly decreases and a new peak is formed at 5 ppm. This band is attributed to protons from $-SiH_3$ groups. After oxidation with N_2O the peak at 5 ppm completely disappears and a broad band at approximately 2.5 ppm appears, indicating the formation of nonacidic protons. These ^{1}H MAS NMR data clearly show that the silane reacts with the acidic protons of the SAPO-34 to form silanols after hydrolysis.

Shown in Figure 6B are the ^{29}Si MAS NMR spectra of the parent SAPO-34 (bottom), the same SAPO-34 after the chemi-

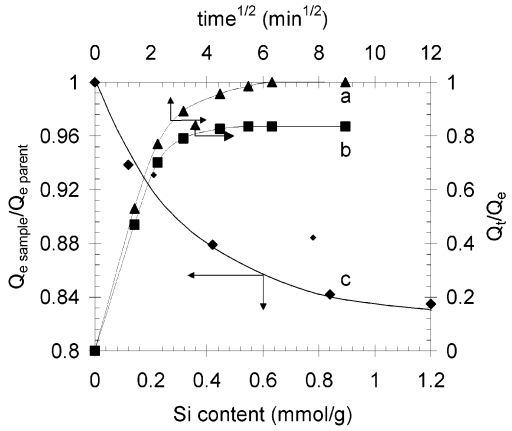

Figure 7. Methanol adsorption kinetics of (a) parent SAPO-34 and (b) Si-modified SAPO-34 (1.2 mmol Si/g SAPO-34). (c) Methanol adsorption capacity as a function of the extra Si content.

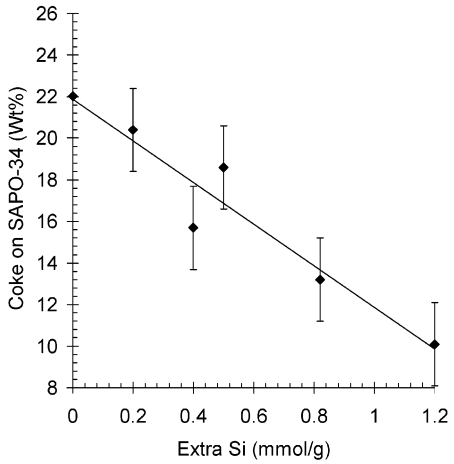

Figure 8. Calculated coke content of SAPO-34 after MTO reaction as a function of the Si content.

sorption of SiH_4 and subsequent hydrolysis (middle), and SAPO-34 after the chemisorption of Si_2H_6 and subsequent hydrolysis (top). The ^{29}Si MAS NMR of the parent shows a distinct peak at −93.5 ppm. This indicates that the Si in the parent SAPO-34 is mainly present as **Si**$(OAl)_4$ and that large Si islands are absent.[26] After the silanation followed by hydrolysis of the Si−H bonds, several new resonances are observed. The peak at −90 ppm is attributed to Si atoms with two neighboring hydroxyl groups. The peaks in the −100 to −120 ppm range arise from the formation of siliceous islands associated with the incorporation of silicon. For example, the peak at approximately −100 ppm is attributed to $(AlO)_3$**Si**(OSi) groups resulting from the reaction of the $(AlO)_3$**Si**−OH−Al acidic group with silane. In this reaction, the acidic Si−O−H reacts with the SiH_4 resulting in a Si−O−Si bond. Similarly, the formation of $(AlO)_2$**Si**$(OSi)_2$ environments leads to intensity in the −107 ppm region. The shift of the **Si**$(OAl)_4$ peak from −93.5 to −95 ppm after reaction with silane is moreover consistent with an increase in silicon content in the second and greater coordination spheres of the framework silicons. These ^{29}Si MAS NMR data confirm that the silane reaction with the acidic protons of the SAPO-34 results in silicon incorporation and silanol formation.

Methanol Uptake. Figure 7 depicts the kinetics of methanol adsorption of the parent sample (a) and of a disilanated SAPO-34 [1.2 mmol Si/g SAPO-34 (b)].

The amount of methanol adsorbed at a time t Q_t relative to the amount adsorbed by the untreated parent sample at equilibrium Q_e is shown as a function of $t^{1/2}$. The data suggest that the methanol adsorption kinetics do not change after modification of the SAPO-34. Even at a modification degree up to 0.6 mmol/g (for Si_2H_6) or 0.78 mmol/g (for SiH_4) the adsorption equilibrium is reached within approximately 30 min, which is the same as for the parent sample. The introduced silyl or disilyl groups however cause a significant decrease in the methanol adsorption capacity (c). Silanation of the SAPO-34 results in a void volume reduction up to 17%, while the highest loading obtained with the disilanation of the samples decreases the void volume up to 25%. The relation between the modification degree and the void volume reduction however is not straightforward.

Catalytic Evaluation. The silanated and disilanated SAPO-34's were tested on their catalytic performance in an MTO reaction. The weighed average product selectivities are summarized in Table 2.

The theoretical amount of coke formed on the SAPO-34 during the MTO reaction was calculated from the difference in H/C ratio of the feed and the products. It was assumed that the H/C ratio of coke is 0.8. The sum of the ethylene and propylene selectivities is 70−75% of the total product selectivity for the parent SAPO-34. Also the (di)silanated SAPO-34 shows high light olefin selectivities. For an extra Si content up to 0.5 mmol/g SAPO-34, only a slight decrease in ethylene + propylene selectivity was observed. When the Si content further increases, the change in ethylene selectivity is more obvious. This is accompanied by an increase in the heavier product selectivity. Remarkably, the propylene selectivity is almost unaffected by the changes in acidity. The ratios ethylene/ethane and propylene/propane however increase with increasing extra Si content. This is caused by a reduction in the Brønsted acidity, which is associated with hydride transfer reactions. The permanent poisoning of strong acid sites suppresses the transformation of olefins to paraffins. These data suggest that there is a relation between the ethylene and the C_4−C_6 selectivities. The distribution between ethylene and C_4−C_6 depends on the total acidity of the SAPO-34, while the propylene selectivity is almost independent of the acidity.

After the MTO reaction, the parent SAPO-34 contained approximately 22 wt % coke, which is the same as the total methanol adsorption capacity. The relation between coke deposition and the (di)silane loading of the SAPO-34 is given in Figure 8. The data suggest a straightforward relation between the extra Si and coke formation. The reduced coke formation is, however, much higher than the reduction in cage volume. This indicates that, after the modification, the SAPO-34 cages are not completely filled with coke during the MTO reaction. The (di)silanation of the Brønsted acid sites results in a reduction of the total acidity. It is therefore proposed that cages where Si was introduced during (di)silanation are not acidic enough to form multiaromatic compounds and the total amount of coke fomed during the conversion of methanol therefore strongly decreases.

Summary

The silanation and disilanation of a TEAOH-templated SAPO-34 has been investigated and the physical and chemical properties of these modified catalysts have been compared with the parent sample. Spectroscopic data show a gradual decrease in the Brønsted acid site density with increasing SiH_4 or Si_2H_6 modification degrees. Simultaneously, an increase in Lewis acid site density was observed by a combined FTIR and CD_3CN desorption study. Catalytic data indicate that the ethylene/ethane and propylene/propane ratios increase with decreasing acidity

of the SAPO-34. The light olefin selectivities are very high for modifications up to 0.5 mmol Si/g SAPO-34. The data suggest a relation between the acidity and the distribution of the ethylene and C_4-C_6 selectivity, while the propylene selectivity is almost independent of the acidity. The coke level decreases with decreasing acidity.

Acknowledgment. F.M. acknowledges ExxonMobil for financial support. P.C. and P.V.D.V. acknowledge the FWO Flanders (Fund for Scientific Research, Flanders, Belgium) for financial support. The assistance of C. E. Chase in recording the NMR data is gratefully acknowledged.

References and Notes

(1) Wilson, S. T.; Lok, B. M.; Messina, C. A.; Cannan, T. R.; Flanigen, E. M. *J. Am. Chem. Soc.* **1982**, *104*, 1146.

(2) Wilson, S. T.; Lok, B. M.; Flanigen, E. M. U.S. Patent 4310440, 1982.

(3) Lok, B. M.; Messina, C. A.; Patton, R. L.; Gajek, R. T.; Cannon, T. R.; Flanigen, E. M. U.S. Patent 4440871, 1984.

(4) Ito, M.; Shimoyama, Y.; Saito, Y. *Acta Crystallogr*. **1985**, *C41*, 1698.

(5) Marchi, A. J.; Froment, G. F. *Appl. Catal.* **1991**, *71*, 139.

(6) Jänchen, J.; Peeters, M. P. J.; van Wolput, J. H. M. C.; Wolthuizen, J. P.; van Hooff, J. H. C. *J. Chem. Soc., Faraday Trans*. **1994**, *90*, 1033.

(7) Chen, J.; Thomas, J. M.; Sankar, G. *J. Chem. Soc., Faraday Trans*. **1994**, *90*, 3455.

(8) Van Niekerk, M. J.; Fletcher, J. C. Q.; O'Connor, C. T. *Appl. Catal. A* **1996**, *138*, 135.

(9) Barrer, R. M.; Vansant, E. F.; Peeters, G. *J. Chem. Soc., Faraday Trans. 1* **1978**, *74*, 1871.

(10) Thijs, A.; Peeters, G.; Vansant, E. F.; Verhaert, I.; De Bièvre, P. *J. Chem. Soc., Faraday Trans I* **1983**, *79*, 2821.

(11) Yan, Y.; Verbiest, J.; Philippaerts, J.; Vansant, E. F.; De Hulsters, P. *Stud. Surf. Sci. Catal.* **1989**, *46*, 759.

(12) Yan, Y.; Vansant, E. F. *J. Phys. Chem*. **1990**, *94*, 2582.

(13) Vansant, E. F. *Pore Size Engineering on Zeolites*; J. Wiley & Sons: New York, 1990.

(14) Pelmenschikov, A. G.; van Santen, R. A.; Jänchen, J.; Meijer, E. *J. Phys. Chem.* **1993**, *97*, 11071.

(15) Barrer, R. M.; Jenkins, R. G.; Peeters, G. In *Molecular Sieves II*; Katzer, J. R., Ed.; ACS Symposium Series 40; American Chemical Society: Washington, DC, 1977; p 285.

(16) Zubkov, S. A.; Kustov, L. M.; Kazansky, V. B. *J. Chem. Soc., Faraday Trans.* **1991**, *87*, 897.

(17) Hegde, S. G.; Ratnasmy, P.; Kustov, L. M.; Kazansky, V. B. *Zeolites* **1988**, *8*, 137.

(18) Pelmenschikov, A. G.; Morosi, G.; Gamba, A.; Coluccia, S.; Martra, G.; Paukshtis, E. A. *J. Phys. Chem.* **1996**, *100*, 5011.

(19) Odinokov, S. E.; Mashkovsky, A. A.; Glasunov, V. P.; Iogansen, A. V.; Rassadin, B. V. *Spectrochim. Acta*, **1976**, *32*, 1355.

(20) Bratos, S. *J. Phys. Chem*. **1975**, *63*, 3499.

(21) Bratos, S.; Ratajczak, H. *J. Chem. Phys*. **1982**, *76*, 77.

(22) Karge, H. G. *Catalysis and Adsorption by Zeolites*; Öhlmann, G., Pfeifer, H., Fricke, R., Ed.; Elsevier: Amsterdam, 1991; p 133.

(23) Sempels, R. E.; Roxhet, P. G. *J. Colloid Interface Sci.* **1976**, *55*, 263.

(24) Venkatesvarlu, P. *J. Phys. Chem*. **1951**, *19*, 293.

(25) Angel, C.; Howell, M. *J. Phys. Chem*. **1969**, *73*, 2551.

(26) Barthomeuf, D. *Zeolites* **1994**, *14*, 394.